Seasonal effects of urban street shading on long-term outdoor thermal comfort

Ruey-Lung Hwang [a], Tzu-Ping Lin [b,*], Andreas Matzarakis [c]

[a] Department of Architecture, National United University, 1 Lien Da, Miaoli 360, Taiwan
[b] Department of Leisure Planning, National Formosa University, 64 Wen-Hua Rd, Huwei, Yunlin 632, Taiwan
[c] Meteorological Institute, Albert-Ludwigs-University Freiburg, Werthmannstr. 10, D-79085 Freiburg, Germany

ARTICLE INFO

ABSTRACT

As shading, an important factor in urban environments, affects thermal environments and long-term thermal comfort, this study conducted several field experiments to analyze the outdoor thermal conditions on urban streets in central Taiwan. The RayMan model was utilized for predicting long-term thermal comfort using meteorological data for a 10-year period. Analytical results indicate that slightly shaded areas typically have highly frequent hot conditions during summer, particularly at noon. However, highly shaded locations generally have a low physiologically equivalent temperature (PET) during winter. Correlation analysis reveals that thermal comfort is best when a location is shaded during spring, summer, and autumn. During winter, low-shade conditions may contribute to the increase in solar radiation; thus, thermal comfort is improved when a location has little shade in winter. We suggest that a certain shading level is best for urban streets, and trees or shade devices should be used to improve the original thermal environment.

1. Introduction

Outdoor thermal comfort of people are affected by thermal environment, moreover, people's usage of outdoors are affected by their perception of outdoor thermal conditions[1–4]. Furthermore, outdoor thermal environments are significantly affected by the design of built environment [5–10]. Since shadings can block direct solar radiation, numerous studies examine the effects of shading on outdoor thermal environments. For instance, previous studies [11–18] quantified the height/width (H/W) ratio of urban streets to assess shading levels, whereas the sky view factor (SVF) was used in other studies as representative of shading levels [19–23].

Ali-Toudert and Mayer, who simulated microclimatic changes by applying the ENVI-met model to an urban environment in Ghardaia, Algeria [15,16], determined that the spatial distribution of physiologically equivalent temperature (PET) at the street level depended strongly on the H/W ratio of urban streets. Emmanuel et al. [13] conducted field experiments at five locations during spring in the city of Colombo, Sri Lanka. They calculated the mean radiant temperature (Tmrt) and PET using the RayMan model [24], and found that deep street canyons (i.e., highly shaded streets) improved the outdoor thermal comfort of pedestrians. Lin et al. [25] indicated that studies with few field experiments can elucidate

characteristics measured (or simulated) on a particular day and likely do not represent annual thermal conditions. Therefore, they conducted several field experiments to analyze outdoor thermal conditions at a university campus in central Taiwan, and employed the RayMan model for predicting long-term thermal comfort using meteorological data for a 10-year period. The thermal comfort range of PETs of Taiwanese residents obtained in a previous study [26] was also applied as the criterion for determining whether a thermal environment is comfortable or uncomfortable.

However, some issues related to shading on urban streets need further clarification. First, previous studies have not discussed the relationship between shading and thermal comfort in different seasons. Since a thermal environment may be comfortable in summer and cold in winter under the same amount of shade, the thermal comfort of a location must be addressed in different seasons. Furthermore, thermal comfort may vary at different times of the day (e.g. hot at noon and cool in the morning); thus, one must also determine the thermal comfort distribution during a given day to elucidate the thermal conditions at different times.

Buildings on Taiwan's traditional streets are mostly residential and commercial, i.e., the first floor is rented by stores and all other floors are residential. If these buildings are not designed with an arcade on the ground floor and lack shading, people must walk beside the street while shopping, and are exposed to the outdoor climate. Thus, people may not be satisfied with their shopping experiences when they feel uncomfortable in an outdoor thermal environment, adversely affecting store revenue and reducing rental

* Corresponding author. Tel.: +886 5 631 5890; fax: +886 5 631 5887.
  E-mail address: tplin@nfu.edu.tw (T.-P. Lin).

prices. Therefore, investigating thermal comfort on urban blocks is essential to the economy.

The aims of this study were to

- conducted field experiment in traditional urban streets in Taiwan;
- establish the prediction model for the thermal environments based on the long-term meteorological data;
- evaluate the long-term thermal comfort frequencies based on the local thermal comfort criteria;
- examine the seasonal effects of urban street shading on long-term outdoor thermal comfort.

2. Research Approach

2.1. Outdoor thermal comfort indices

Several indices that integrate thermal factors based on the energy balance of the human body, SET* [27], OUT_SET* [28] and PET [29], are employed in assessing outdoor thermal comfort. Notably, PET is defined as air temperature (Ta) at which, in a typical indoor setting (Ta = Tmrt; vapor pressure (Vp) = 12 hpa; and wind speed (v) = 0.1 m/s), the heat budget of the human body is balanced with the same core and skin temperature as those under complex outdoor conditions [30,31]. In this study, we apply PET for the main thermal comfort index for the following reasons.

The first reason is that PET have been employed in several studies of outdoor thermal comfort [32–34] and is included in guideline 3787 of the German Association of Engineers (VDI) [29]. Furthermore, the thermal comfort criteria of PET have been modified and adopted setup for different climate regions [26,35].

The second reason is that PET can be estimate by the RayMan model, has been utilized in urban built-up areas and to generate predictions of thermal comfort in outdoor environments [24,36–38]. Lin et al. [25] indicated that the PET can be easily estimated by Ta, relative humidity (RH) (or Vp), v, Tmrt, human

clothing and activity in the model. If more information is offered, the Tmrt (the most important factor during hot condition when calculating PET) can be also estimated by global radiation (Gr), cloud cover (Cd), fisheye photographs, albedo, the Bowen ratio of ground surface and the Linke turbidity to include the shading effect while calculating short- and long-wave radiation fluxes. Besides PET and Tmrt, the sky view factor (SVF), i.e. the ratio of free sky spaces to the entire fisheye view at a certain location, can also be calculated using the RayMan model for subsequent analyses.

2.2. Local thermal comfort criterion for PET

Previous studies examining thermal adaptation indicated that occupant thermal sensations and preferences vary considerably due to differences in behavioral adjustment, physiological acclimatization, and psychological habituation or expectations [39], all of which may contribute to different thermal comfort ranges, i.e., the range of thermal indices at which people feel comfortable. Therefore, the thermal comfort range for a particular region may not be applicable to other regions. In this study, the thermal comfort range is acquired from a field survey of 1644 subjects in Taiwan [26]. In this survey, 26–30 °C PET was the "neutral" sensation, 18–22 °C PET was "slightly cool", 14–18 °C PET was "cool", and <14 °C PET was "cold"; additionally, 30–34 °C PET was "slightly warm", 34–38 °C PET was "warm", 38–42 °C PET was "hot", and >42 °C PET was "very hot". As these thermal comfort ranges have been applied generally in Taiwan, a hot and humid country [25], these thermal comfort ranges are applied as criteria in this study to determine whether a thermal environment is comfortable or uncomfortable for local residents.

2.3. The field experiment

This study chose streets for measurements that are almost walking spaces and with many commercial businesses (e.g.,

Fig. 1. Studied area and measurement locations in Huwei Township.

Table 1
Fisheye and street photographs and the SVF of each measurement location.

Fisheye photo	Street photo	SVF
A		0.236
B		0.309
C		0.326
D		0.348
E		0.555
F		0.616
K		0.879

restaurants and stores) and were not interfered with by traffic or huge air-conditioners. Therefore, a traditional street in Huwei Township, located at 23°43′ N, 120°26′ E at an elevation of 20 m above sea level, was selected. Fig. 1 shows the area surveyed in this study. Measurement locations A–F, which are outdoor spaces most frequently used by local residents, are characterized by different shading levels. Point K, a reference for locations A–F, is located on the roof of a 10 m-high building with no shade.

Table 1 shows fisheye and street photographs and the SVF of each measurement location. Among the six measurement locations, the SVF ranges from highly shaded—point A (SVF = 0.236)—to slightly shaded—point F (SVF = 0.616) (Table 1).

To measure physical thermal parameters, survey instruments were placed at 1.1 m above ground level on a tripod at locations A–F and K to measure Ta, RH, and globe temperature (Tg). At location K, v and Gr were also measured simultaneously. Measurements were recorded at 1-min intervals automatically from 08:00 to 18:00, as this is the period when shoppers are outdoors most; thus, this period is also the period used in subsequent analyses. Four field experiments were conducted, one in each season, to ensure data representativeness of climate characteristics in each season.

2.4. Validation of RayMan model

The RayMan model must be validated by comparing field measurements and model simulation results to fit the local climate and urban context. Since Tmrt is an integrated thermal index representing the combination of Ta, v, and short- and long-wave radiation fluxes, and can be determined via both measurements and simulations, the consistency between measured and modeled Tmrt was utilized as a criterion for model validation. The measured Tmrt was calculated using Ta, Tg, and v based on ISO standard 7726 [40]. The mean convection coefficient was corrected using the method developed by Thorsson et al. [41]. The modeled Tmrt was calculated using the RayMan model by importing the same factors used in calculating PET. According to the method applied in Lin et al. [25], Tmrt for each location is estimated by Gr, cloud cover, fisheye photographs and other climatic and environmental factors during the experiments.

2.5. Simulation of long-term thermal environment conditions

Long-term meteorological data from weather stations were imported into the model with optimal settings for predicting long-term variations in thermal environmental conditions and thermal indices. The meteorological hourly data for the 10-year period of 2000–2009 utilized in this study acquired were from the nearest weather station; this weather station is in Chiayi. The Ta, RH, v, Gr, and Cd of hourly data were imported into the RayMan model. Since meteorological data were not acquired in the surveyed area and cannot directly represent the thermal conditions at measurement locations A–F, we assume the thermal conditions at measurement locations are related to meteorological data, and these data must be corrected before being imported into the model.

For estimations of thermal conditions at each location, as the closest weather station is near Huwei Township, and the slightly shaded location K has as a height and sky conditions similar to those at the weather station, climate data at K were assumed close to those measured at the weather station. According to the method used in Lin et al. [25], the long-term Ta, v, and Gr for each locations is then modified by climate data of weather station based on regression analysis. The regressive functions of Ta for each location are highly correlated to experimental result (R^2 = 0.92–0.96, p-value < 0.001) in this study.

Table 2
Mean values of physical measurements for location K on each measurement day. Values in parentheses are minimum and maximum.

Season	Date	Air temperature (°C)	Relative humidity (%)	Wind speed (m/s)	Global radiation (W/m²)
Winter	2009/1/11	16.9 (9.3–20)	53.9 (46.3–72.7)	1.4 (0.6–2.3)	402.5 (0–671.4)
Spring	2009/3/22	29.7 (25.9–32.6)	65.8 (54.1–82.2)	2.2 (0.6–3.6)	423.8 (43.6–808.2)
Summer	2009/8/1	34.2 (30.1–36.4)	61.6 (53.6–82.1)	0.9 (0.3–1.6)	535.6 (125.5–953.2)
Autumn	2008/10/18	32.2 (27.9–35.9)	64 (48–80)	0.7 (0.3–1.7)	469.3 (5–913.4)

3. Results and discussion

3.1. Field experiment results and model validation

Field experiments were conducted on January 11, 2009, during winter, on March 22, 2009, during spring, on August 1, 2009, during summer, and on October 18, 2008, during autumn. Measurements were recorded from 08:00 to 18:00 on each day. For location K (Table 2), mean Ta in winter was <20 °C, while Ta in the other seasons was >30 °C. The average RH was 54–64% and average wind speed at each measured day was <2.5 m/s. Average Gr was 400–600 W/m²; the highest Gr values in summer, spring, and autumn were always >800 W/m². These data characterize the local climate as hot in summer and mild in winter with high humidity all year.
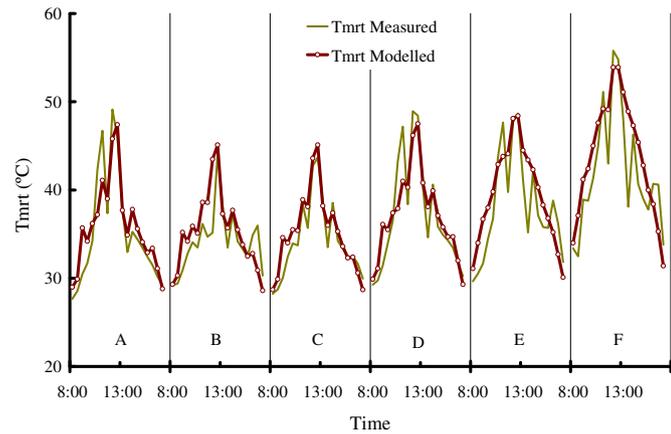
Fig. 2 shows the variation in both measured and modeled Tmrt for cases in spring (March 22, 2009). The modeled Tmrt and measured Tmrt have similar trends and values. The measured Tmrt and modeled Tmrt were strongly correlated ($R^2 = 0.88$, $P < 0.001$) (Fig. 3), demonstrating that the model is accurate in predicting Tmrt and PET.
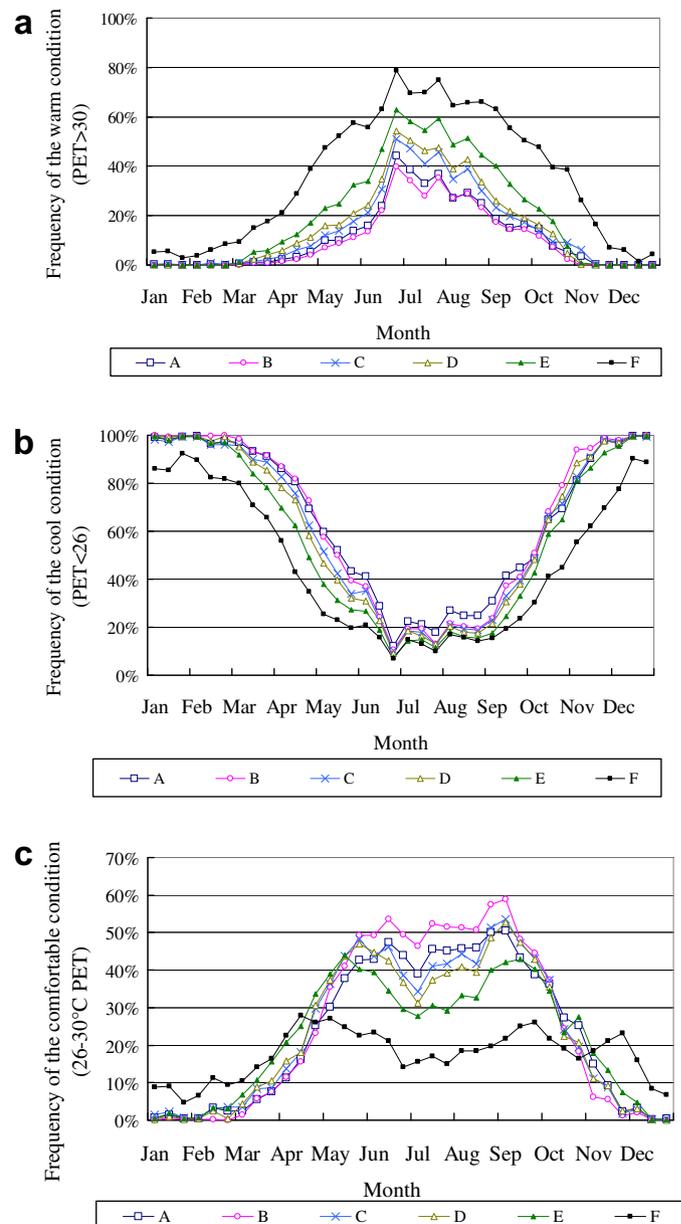

Fig. 2. Variation in both measured and modeled Tmrt for cases in spring (March 22, 2009).

$y = 0.9557x + 1.9751$
$R^2 = 0.8834$
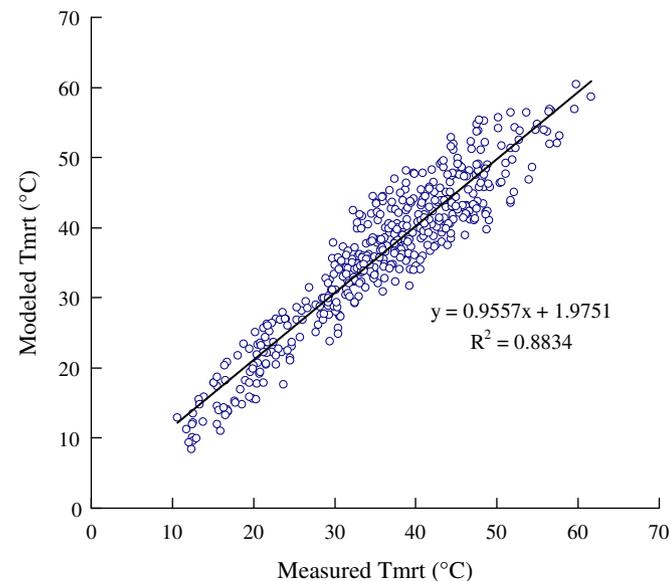
Fig. 3. Correlation between measured and modeled Tmrt.

Fig. 4. Predicted frequencies for the warm condition (a), cool condition (b) and thermal comfort condition (c) at 08:00–18:00, 2000–2009.

3.2. Long-term thermal perceptions frequencies

According to the assumptions and prediction method discussed in Section 3.3, meteorological data were corrected and imported into the model to derive hourly PET over the last 10 years. While expressing the calculated PET, the frequencies of three thermal sensation classifications were calculated based on the thermal comfort range in Taiwan. The first is the frequency of the warm condition; that is, the percentage of warm hours (PET > 30 °C) over total hours during a specific period, which is expressed as $F_{PET>30}$ (Fig. 4(a)). The second is the frequency of the cool condition, i.e., $F_{PET<26}$ (Fig. 4(b)), and the third is the frequency of the comfortable condition, i.e., $F_{26<PET<30}$ (Fig. 4(c)). These three frequencies are calculated using hourly data for the 10-year period of 2000–2009 and are presented in 10-day intervals (36 intervals/year) to increase data resolution. Since the original field experiment time and model validation period are both during 8:00–18:00, long-term simulation results are more reliable during 8:00–18:00 than the rest time of a day. Therefore, we only displayed the simulation results between 8:00–18:00 in this study.

The $F_{PET>30}$ was high in summer and low during the other seasons for all locations (Fig. 4(a)). The $F_{PET>30}$ values for highly shaded locations (i.e., A and B) were <40% throughout the whole year, while that of the slightly shaded location (i.e., F) was >60% during June to August. However, the $F_{PET<26}$ was low in summer, spring, and fall and high in winter at all locations (Fig. 4(b)). The $F_{PET<26}$ values for highly shaded locations (i.e., A and B) were close to 100% during winter, while that for slightly shaded location F was much lower than those for the remaining locations during winter, spring, and autumn.

The $F_{26<PET<30}$ of the slightly shaded location, F, was 10–30% all year, while that of the highly shaded locations, A, and B, was high in summer and low in winter (Fig. 4(c)). This is because the warm condition at these highly shaded locations seldom occurred during summer ($F_{PET>30}$ < 40%) and cool conditions were extremely frequent during winter ($F_{PET<26}$ almost 100%); thus, thermal comfort peaked in summer and was rare in winter at highly shaded locations. Therefore, different shading levels contribute to the variation in the thermal perception distribution.

3.3. Mean thermal sensations at different periods in a day

However, the frequency of each thermal perception acquired in the previous sections is difficult to use when interpreting thermal comfort variations during a given day (e.g., differences between morning and afternoon). Since several studies revealed that there are significant time-induced effects on thermal comfort or user response under a changing conditions within a day [11,15,31], this study generated the PET isotherm for each location for further elucidation. Fig. 5 shows a PET isotherm, where the *x*-coordinate refers to the month and the *y*-coordinate is time. This study calculated PET averages for different times for each 10-day period using PET data for 2000–2009. For example, PET at 8:00 on Jan. 1–10 was the average of 100 climate data (10 year × 10 days) at 8:00 from Jan. 1 to 10 in 2000–2009. Based on this principle, this study calculated PET and generated the PET isotherm using the Kriging algorithm in the Surfer® program.

This study chose three locations with different levels of shading to determine their PET isotherm, i.e., highly shaded A (SVF = 0.236),
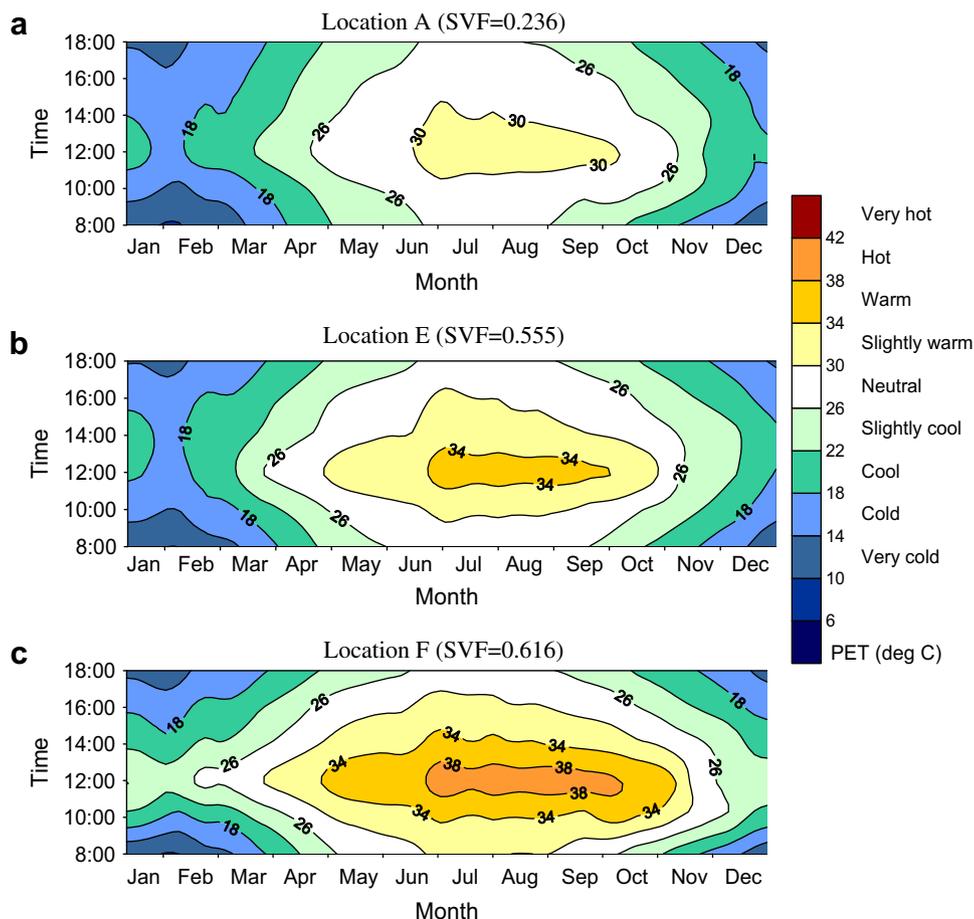

Fig. 5. Predicted PET isotherm for locations A(a), E(b), and F(c), 2000–2009.

moderately shaded E (SVF = 0.555) and slightly shaded F (SVF = 0.616). For location A (Fig. 5(a)), the thermal comfort period (white) was from July to September except at noon, and at noon during May, June, and October. "Slightly warm" (PET > 30 °C) was at noon during July to September. "Slightly cool" (PET < 26 °C) was distributed from November to April. For location E (Fig. 5(b)), the "thermal comfort" period was shorter and the "slightly warm" period was longer than those at location A. "Slightly warm" was

distributed from May to October, and "warm" occurred from July to September. For the slightly shaded location, F (Fig. 5(c)), "slightly warm" was widely distributed during March to November, almost reaching "hot" at noon during July to September. Therefore, the thermal sensation distribution varied at different periods in a day, revealing that the slightly shaded areas are hot at noon in summer while highly shaded areas are more comfortable throughout the whole year.

3.4. The correlation between SVF and thermal comfort for each season

To assess the correlation between the SVF on urban streets in different seasons, this study analyzed the frequency of the warm condition ($F_{PET>30}$) and frequencies of the cool condition ($F_{PET<26}$) and comfortable condition ($F_{26<PET<30}$) at each location on urban streets during different seasons. First, these three frequencies at each location were calculated for each season and their SVF values were plotted (Fig. 6(a)–(c)), and fitted with a regression line for each season. The positive or negative slope of each regression line indicates whether the correlation between the SVF and frequencies are positive or negative, while the absolute value of the slope shows the sensitivities of frequencies to variation in the SVF.

The correlation between the SVF and $F_{PET>30}$ was positive, i.e., locations with a high SVF (slightly shaded) were hot (Fig. 6(a)). Based on the slope of the four fitted lines, the value in summer was highest, spring and autumn had a moderate value, while winter had the lowest value. These analytical results reveal that the $F_{PET>30}$ is more sensitive to variation in the SVF in hot seasons than in cool seasons. Furthermore, $F_{PET>30}$ was the highest in summer given the same SVF value for the same location.

The correlation between SVF and $F_{PET<26}$ was negative, i.e., locations with a low SVF (highly shaded) were cool (Fig. 6(b)). Based on the slope of the four fitted lines, the values for spring and autumn were highest. Analytical results demonstrate that the $F_{PET<26}$ was more sensitive to the variation in the SVF in spring and autumn than in summer and winter. Furthermore, $F_{PET<26}$ was highest in winter given the same SVF value for the same location.

The correlation between the SVF and $F_{26<PET<30}$ was negative in winter and positive in the other seasons, i.e., locations with a high SVF are comfortable in winter and uncomfortable in other seasons (Fig. 6(c)).

These experimental results reveal some important phenomena. First, shaded locations have fewer warm hours, especially in summer, than non-shaded locations. The elevation of the sun is high at noon in summer, which increases the likelihood of sunlight directly hitting the street, likely accounts for this finding. Conversely, locations with considerable shading increase the duration of cool hours. When the comfort condition is evaluated, highly shaded areas are beneficial in spring, summer, and autumn, while minimal shade is comfortable only in winter as increased sunlight (solar radiation) overcomes the original cool-air condition. Therefore, the effects of shading vary in different seasons.

4. Conclusions

This study focused on six locations on urban streets in Huwei Township, central Taiwan, and discussed the effects of shading on long-term outdoor thermal comfort and seasonal variation. Four field experiments were conducted during each season to establish and validate the RayMan model for the simulation of the long-term thermal comfort based on 10-year meteorological data. The thermal comfort criterion of Taiwanese residents obtained in a previous survey was applied as the criterion for determining whether a thermal environment is comfortable or uncomfortable.
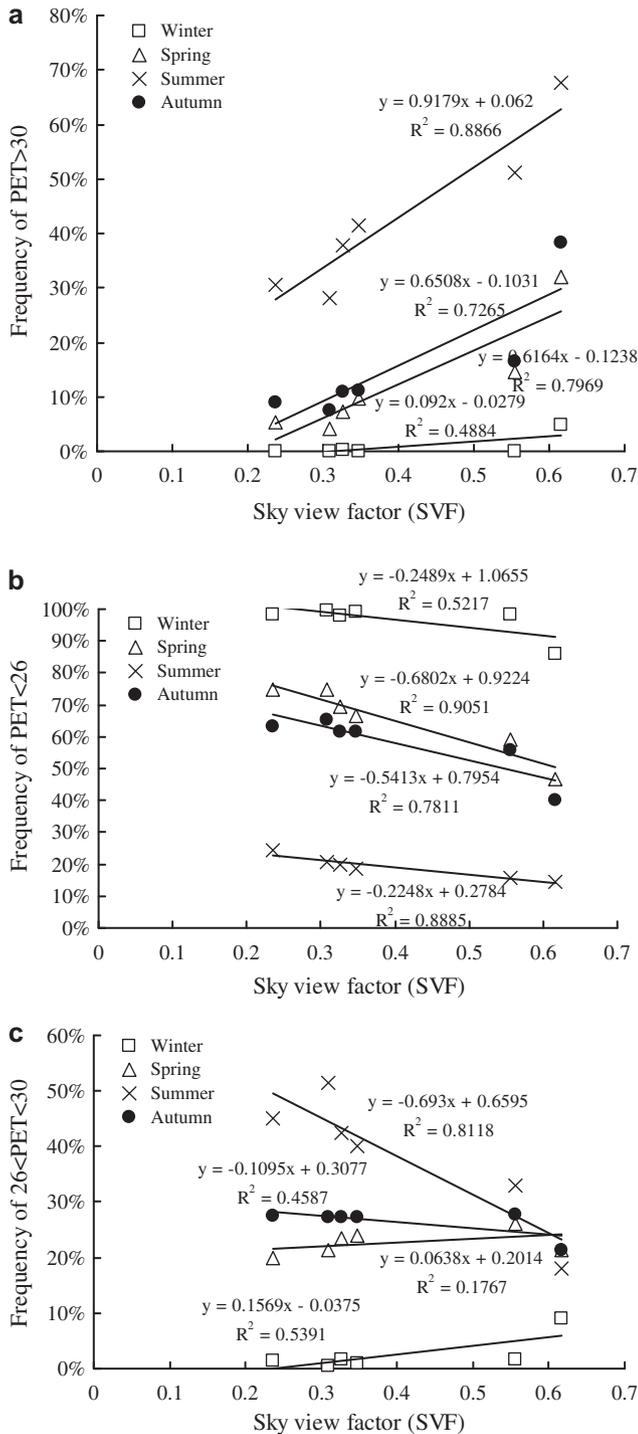

Fig. 6. Correlation between the SVF and frequencies of the warm condition (a), cool condition (b) and comfort condition (c) at each location on urban streets in different seasons.

Concerning the issue of responding time of PET in the fluctuating microclimate, it should be discussed and clarified in two stage of this research. The first part is filed experiment and model validation (section 3.2 and 3.3), due to the 1-min interval measured data is collected, the calculated PET can actually response the fluctuating change in microclimate. The second stage is Long-term simulation (3.3). Due to the available climate data is 1-h interval, the hourly data are imported to the RayMan model the calculated the long-term PET. In this research, the purpose of the long-term simulation is to describe the frequencies thermal perceptions roughly, instead of displaying the instantaneous change in microclimate precisely. Since each thermal perception is ranged about 4 °C (e.g. thermal comfort is 28–30 °C PET), distribution differences of thermal perception frequencies caused by the slightly microclimate fluctuating are relatively small. Furthermore, PET values based on hourly data have been used to predicted thermal comfort for many studies [15,42–45]. To sum up, we think PET index is adequate to be used in dealing with either instantaneous dynamic outdoor thermal conditions or long-term (e.g. daily, seasonally, annually) thermal condition based on hourly climate data.

Analytical results indicate that slightly shaded locations typically have high frequency hot conditions in summer, especially at noon. However, highly shaded locations tend to have a relatively lower PET in winter. Correlation analysis reveals that thermal comfort is best when a location is shaded in spring, summer, and autumn. In winter, the slightly shaded condition may contribute to increased solar radiation; thus, thermal comfort is best when a location has little shade.

Since the thermal comfort condition varies in different seasons, we cannot suggest a certain shading level or H/W ratio for urban streets. Furthermore, the heights of new buildings are always restricted by land use policy in urban areas and old buildings are hard to re-build. However, study results may have some significant applications. For example, some shading devices on urban streets may be added in summer and removed in winter. Additionally, deciduous trees may prove helpful in providing shade in summer and letting solar radiation enter streets in winter.

Acknowledgements

References

[1] Nikolopoulou M, Baker N, Steemers K. Thermal comfort in outdoor urban spaces: understanding the human parameter. Solar Energy 2001;70:227–35.
[2] Thorsson S, Lindqvist M, Lindqvist S. Thermal bioclimatic conditions and patterns of behaviour in an urban park in Goteborg, Sweden. International Journal of Biometeorology 2004;48:149–56.
[3] Eliasson I, Knez I, Westerberg U, Thorsson S, Lindberg F. Climate and behaviour in a Nordic city. Landscape and Urban Planning 2007;82:72–84.
[4] Lin TP. Thermal perception, adaptation and attendance in a public square in hot and humid regions. Building and Environment 2009;44:2017–26.
[5] Lin TP, Ho YF, Huang YS. Seasonal effect of pavement on outdoor thermal environments in subtropical Taiwan. Building and Environment 2007;42: 4124–31.
[6] Tan SA, Fwa TF. Influence of pavement materials on the thermal environment of outdoor spaces. Building and Environment 1992;27:289–95.
[7] Taha H. Urban climates and heat islands: albedo, evapotranspiration, and anthropogenic heat. Energy and Buildings 1997;25:99–103.
[8] Asaeda T, Ca VT. Characteristics of permeable pavement during hot summer weather and impact on the thermal environment. Building and Environment 2000;35:363–75.
[9] Wong NH, Jusuf SK, La Win AA, Thu HK, Negara TS, Wu XC. Environmental study of the impact of greenery in an institutional campus in the tropics. Building and Environment 2007;42:2949–70.
[10] Ichinose T, Shimodozono K, Hanaki K. Impact of anthropogenic heat on urban climate in Tokyo. Atmospheric Environment 1999;33:3897–909.
[11] Johansson E. Influence of urban geometry on outdoor thermal comfort in a hot dry climate: a study in Fez, Morocco. Building and Environment 2006;41: 1326–38.
[12] Johansson E, Emmanuel R. The influence of urban design on outdoor thermal comfort in the hot, humid city of Colombo, Sri Lanka. International Journal of Biometeorology 2006;51:119–33.
[13] Emmanuel R, Johansson E. Influence of urban morphology and sea breeze on hot humid microclimate: the case of Colombo, Sri Lanka. Climate Research 2006;30:189–200.
[14] Ali-Toudert F, Mayer H. Thermal comfort in an east–west oriented street canyon in Freiburg (Germany) under hot summer conditions. Theoretical and Applied Climatology 2007;87:223–37.
[15] Ali-Toudert F, Mayer H. Numerical study on the effects of aspect ratio and orientation of an urban street canyon on outdoor thermal comfort in hot and dry climate. Building and Environment 2006;41:94–108.
[16] Ali-Toudert F, Mayer H. Effects of asymmetry, galleries, overhanging facades and vegetation on thermal comfort in urban street canyons. Solar Energy 2007;81:742–54.
[17] Emmanuel R, Rosenlund H, Johansson E. Urban shading – a design option for the tropics? A study in Colombo, Sri Lanka. International Journal of Climatology 2007;27:1995–2004.
[18] Shashua-Bar L, Potchter O, Bitan A, Boltansky D, Yaakov Y. Microclimate modelling of street tree species effects within the varied urban morphology in the Mediterranean city of Tel Aviv, Israel. International Journal of Climatology 2010;30:44–57.
[19] Giridharan R, Lau SSY, Ganesan S. Nocturnal heat island effect in urban residential developments of Hong Kong. Energy and Buildings 2005;37: 964–71.
[20] Bottyan Z, Unger J. A multiple linear statistical model for estimating the mean maximum urban heat island. Theoretical and Applied Climatology 2003;75: 233–43.
[21] Hamdi R, Schayes G. Sensitivity study of the urban heat island intensity to urban characteristics. International Journal of Climatology 2007;28: 973–82.
[22] Giridharan R, Lau SSY, Ganesan S, Givoni B. Urban design factors influencing heat island intensity in high-rise high-density environments of Hong Kong. Building and Environment 2007;42:3669–84.
[23] Dimoudi A, Nikolopoulou M. Vegetation in the urban environment: microclimatic analysis and benefits. Energy and Buildings 2003;35:69–76.
[24] Matzarakis A, Rutz F, Mayer H. Modelling radiation fluxes in simple and complex environments – application of the RayMan model. International Journal of Biometeorology 2007;51:323–34.
[25] Lin TP, Matzarakis A, Hwang RL. Shading effect on long-term outdoor thermal comfort. Building and Environment 2010;45:213–21.
[26] Lin TP, Matzarakis A. Tourism climate and thermal comfort in Sun Moon Lake, Taiwan. International Journal of Biometeorology 2008;52:281–90.
[27] Gagge AP, Fobelets AP, Berglund LG. A standard predictive index of human response to the thermal environment. ASHRAE Transactions 1986;92:709–31.
[28] Spagnolo J, de Dear RJ. A field study of thermal comfort in outdoor and semi-outdoor environments in subtropical Sydney Australia. Building and Environment 2003;38:721–38.
[29] VDI. Methods for the human biometeorological evaluation of climate and air quality for the urban and regional planning. Part I: climate. VDI guideline 3787. Part 2. Berlin: Beuth; 1998.
[30] Höppe P. The physiological equivalent temperature – a universal index for the biometeorological assessment of the thermal environment. International Journal of Biometeorology 1999;43:71–5.
[31] Mayer H, Höppe P. Thermal comfort of man in different urban environments. Theoretical and Applied Climatology 1987;38:43–9.
[32] Thorsson S, Honjo T, Lindberg F, Eliasson I, Lim EM. Thermal comfort and outdoor activity in Japanese urban public places. Environment and Behavior 2007;39:660–84.
[33] Andrade H, Alcoforado M-J. Microclimatic variation of thermal comfort in a district of Lisbon (Telheiras) at night. Theoretical and Applied Climatology 2007;92:225–37.
[34] Oliveira S, Andrade H. An initial assessment of the bioclimatic comfort in an outdoor public space in Lisbon. International Journal of Biometeorology 2007;52:69–84.
[35] Matzarakis A, Mayer H. Another kind of environmental stress: thermal stress. WHO Collaborating Centre for air Quality Management and air Pollution Control. Newsletters 1996;18:7–10.
[36] Gulyas A, Unger J, Matzarakis A. Assessment of the microclimatic and human comfort conditions in a complex urban environment: modelling and measurements. Building and Environment 2006;41:1713–22.
[37] Lin TP, Matzarakis A, Huang JJ. Thermal comfort and passive design of bus shelters. In: Proceedings of 23rd conference on passive and low energy architecture (PLEA2006); 2006. Geneva.

[38] Matzarakis A, Rutz F, Mayer H. Modelling radiation fluxes in simple and complex environments: basics of the RayMan model. International Journal of Biometeorology 2010;54:131–9.

[39] Brager GS, de Dear RJ. Thermal adaptation in the built environment: a literature review. Energy and Buildings 1998;27:83–96.

[40] ISO. International standard 7726, thermal environment-instruments and method for measuring physical quantities. Geneva: International Standard Organization; 1998.

[41] Thorsson S, Lindberg F, Eliasson I, Holmer B. Different methods for estimating the mean radiant temperature in an outdoor urban setting. International Journal of Climatology 2007;27:1983–93.

[42] Zaninovic K, Matzarakis A. The bioclimatological leaflet as a means conveying climatological information to tourists and the tourism industry. International Journal of Biometeorology 2009;53:369–74.

[43] Thorsson S, Eliasson I. An intra-urban thermal breeze in Goteborg, Sweden. Theoretical and Applied Climatology 2003;75:93–104.

[44] Svensson M, Eliasson I. Diurnal air temperatures in built-up areas in relation to urban planning. Landscape and Urban Planning 2002;61: 37–54.

[45] Mayer H, Holst J, Dostal P, Imbery F, Schindler D. Human thermal comfort in summer within an urban street canyon in Central Europe. Meteorologische Zeitschrift 2008;17:241–50.